Solvent Extraction Research and Development, Japan, **Vol. 30, No 1, 1 – 12 (2023)**

Synthesis of Crosslinked Poly(Vinylphosphonic Acid) Particles by Water-in-Oil (W/O) Suspension Polymerization Method and Their Adsorption Properties of Metal Ions

Benny Rio FERNANDEZ[1,2] and Satoshi TSUKAHARA[1,*]

[1]*Department of Chemistry, Graduate School of Science, Osaka University, 1-1, Machikaneyama, Toyonaka, Osaka 560-0043, Japan;* [2]*Departmen of Palm Oil Agrobusiness, Politeknik Teknologi Kimia Industri (PTKI)-Medan, Jln. Medan Tenggara VII, Kec. Medan Denai, Medan City, North Sumatera 20228, Indonesia*

** Corresponding author: sxt@chem.sci.osaka-u.ac.jp*

(Received January 30, 2022; Accepted March 30, 2022)

Crosslinked poly(vinylphosphonic acid) (PVPA) particles were successfully synthesized from vinylphosphonic acid and a crosslinker by water-in-oil (W/O) suspension polymerization using three silicone oils. The structure, morphology, and size of the PVPA particles were confirmed by Fourier transform infrared spectroscopy, scanning electron microscopy, and optical microscopy. The surface of the spherical particles was wrinkled, and their size ranged from 5 – 260 μm. The adsorption of divalent and trivalent metal ions (Cu^{2+}, Zn^{2+}, La^{3+}, Tb^{3+}, Lu^{3+}) from aqueous solutions was studied using the synthesized PVPA particles under batch conditions at various metal ion concentrations and pHs for the first time. For all metal ions, pH-dependent adsorptions were observed. Partial charge neutralization of metal ions occurred because the PVPA particles are highly hydrophilic. The extraction efficiencies of La^{3+}, Tb^{3+}, and Lu^{3+} are higher than those of Cu^{2+} and Zn^{2+}. The separation ability for La^{3+}, Tb^{3+}, and Lu^{3+} is not so high, but they can be used for the group extraction of these metal ions.

1. Introduction

Functionalized microparticles are one of the important synthetic polymers and have been used in many applications, such as cosmetics [1], biomedicine [2], coatings [3], drug delivery system [4], agriculture [5], and chemical separation [6-8]. As for the concentration or recovery of metal ions, ion-exchange resin particles have been widely used in various fields. Compared with solvent extraction, the technique using particles has the advantages of easier stirring and easier phase separation. However, there are insufficient studies on the synthesis of particles with new functional groups and the adsorption of metal ions onto these particles.

Phosphoric acid diester or alkylphosphonic acid monoester is one of the promising extractants that have been used in the solvent extraction of metal ions. Among these, di(2-ethylhexyl) hydrogen phosphate (D2EHPA) and 2-ethylhexyl hydrogen 2-ethylhexylphosphonate (PC88A) are particularly famous and have been widely studied [9-11]. In coordination chemistry, ligands containing phosphorous are also well known. However, particles with phosphoric acid groups or phosphonic acid groups are not widely known.

One of the particles with phosphonic acid groups is poly(vinylphosphonic acid) (PVPA) and its derivatives. Kaltbeitzel *et al.* reported the synthesis of PVPA and used it for water adsorption [12]. Najafi *et al.* designed PVPA particles for alcohol adsorption [13]. Kwak *et al.* prepared PVPA-based microgels and used them for In^{3+} adsorption [14,15]. Sahiner *et al.* synthesized PVPA microgels for uranyl adsorption [16].

Anil *et al*. reported dyes adsorption onto crosslinked PVPA [17]. However, the existing literature indicates that there is no report on the adsorption capabilities of PVPA-based particles for transition metal ions and lanthanoid ions.

Four heterogeneous polymerization methods are known at present: emulsion polymerization, dispersion polymerization, precipitation polymerization, and suspension polymerization [18]. The emulsion polymerization is an effective method to make small and monodispersed spherical particles using surfactants, but the surfactants would remain on the particle surface. The dispersion and precipitation polymerizations are not suitable for the purpose of the present study because they are methods involving the solid phase. The suspension polymerization is a method that uses a stabilizer instead of a surfactant. It makes larger particles (10 μm – 5 mm in size) than the emulsion polymerization, but this method has the advantages that surface modification is possible and surfactants do not remain on the surface [18,19]. Numerous reports on the preparation of particles by the suspension polymerization have been published in the literatures [20,21]. We employed the suspension polymerization method because we wanted to have a large number of phosphonic acid groups present on the surface without surfactant interference.

In the present study, we targeted particles possessing phosphonic acid groups. To synthesize them by the W/O suspension polymerization method, vinylphosphonic acid (VPA) was selected as the main monomer because it is soluble in water and it has sufficient polymerization reactivity. Poly(ethylene glycol) diacrylate (PEGDA) was selected as the crosslinker because it is also soluble in water and it has no functional groups that interact with metal ions electrostatically. The chemical structures of VPA and PEGDA are shown in Scheme 1. The crosslinker leads to the formation of a three-dimensional network and the formation of pores in PVPA particles [22]. To increase the number of the functional groups (phosphonic acid groups), the VPA content should be high. Adsorption properties of divalent metal ions (Cu^{2+} and Zn^{2+}) and trivalent metal ions (La^{3+}, Tb^{3+}, and Lu^{3+}) were studied by using the synthesized PVPA particles. We selected Cu^{2+} and Zn^{2+} because they are typical divalent metal ions, and we selected La^{3+}, Tb^{3+}, and Lu^{3+} because phosphoric acid diester or alkylphosphonic acid monoester has a high extraction efficiency and high separation ability for lanthanoid ions.

2. Experimental

2.1 Reagents

VPA (95% purity), benzoyl peroxide (BPO; 75% purity), and 2-ethyl-1,3-hexanediol (purity $\geq$ 98%), were purchased from Tokyo Chemical Industry Co., Ltd. PEGDA (number average molecular weight (M_n) 250) and poly(vinyl alcohol) (PVA; M_n 89,000 – 98,000, 99% hydrolyzed) were obtained from Sigma–Aldrich Co. The average number of ethylene glycol groups of PEGDA was calculated to be 3 from the M_n value. Silicone oils (KF-96-100CS, KF-96-1000CS, and KF-96-3000CS) were purchased from Shin-Etsu Chemical Co., Ltd. Colorimetric complexing reagents, 2-(5-bromo-2-pyridylazo)-5-(*N*-propyl-*N*-sulfopropylamino)phenol disodium salt (5-Br-PAPS) and 2,7-bis(4-chloro-2-phosphonophenylazo)-1,8-dihydroxy-3,6-napthalene disulfonic acid (Chlorophosphonazo-III, CPA-III) were purchased from Dojindo Laboratories (Kumamoto, Japan). $CuCl_2$ (purity 98%), $ZnSO_4 \cdot 7H_2O$ (purity 99.5%), $LaCl_3 \cdot 7H_2O$ (99.9% purity), $TbCl_3 \cdot 6H_2O$ (99.9% purity), $LuCl_3 \cdot 6H_2O$ (99.99% purity), toluene (purity 99.5%), cyclohexanol (purity 98%), and NaOH were obtained from Fujifilm Wako Pure Chemical Co. (Osaka, Japan). K_2HPO_3,

KH_2PO_3, and hydrochloric acid were purchased from Nacalai Tesque, Inc. (Kyoto, Japan). Ultrapure water was made by a Direct-Q UV (Millipore, Merck).

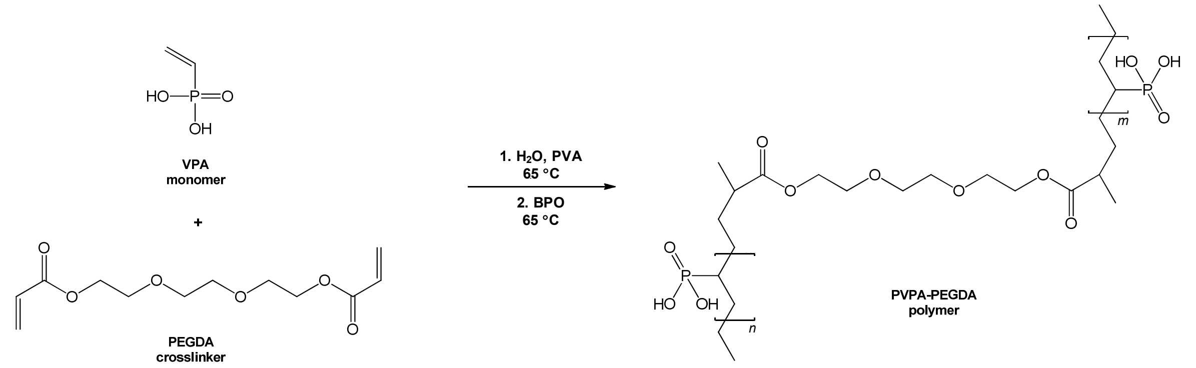

Scheme 1. Reaction scheme of crosslinked PVPA particles.

2.2 Synthesis of crosslinked poly(vinylphosphonic acid) particles

Scheme 1 and Figure 1 show the reaction scheme of crosslinked PVPA and the illustration of the W/O suspension polymerization, respectively. The polymerization was conducted in a 500 mL three-neck round-flask equipped with a magnetic stirrer, a condenser, a nitrogen gas inlet, and a thermometer. The initiator, BPO, was dissolved in 20 mL of toluene, cyclohexanol, or 2-ethyl-1,3-hexanediol. In the case of silicone oils, not all BPO was soluble but the suspension was used as it was. This BPO solution or BPO suspension was first added to the flask with stirring at 400 rpm under nitrogen gas for 10 min (Figure 1(a)). VPA, PEGDA, and PVA were dissolved in 4 mL water at 65 °C, and then this aqueous solution was dropped into the continuous phase (Figure 1(b)) to form water-in-oil (W/O) suspension. Since BPO is hydrophobic and almost insoluble in water, it would work as an initiator at the interface of the W/O suspension (Figure 1(c)). The polymerization was performed at 65 °C for 2 – 3 h under nitrogen gas (Figure 1(d)). The solution was centrifuged at 4000 rpm for 10 – 30 min after polymerization to isolate the particles. The precipitated particles were washed with ethanol and water several times. After that, the particles were dried under vacuum.

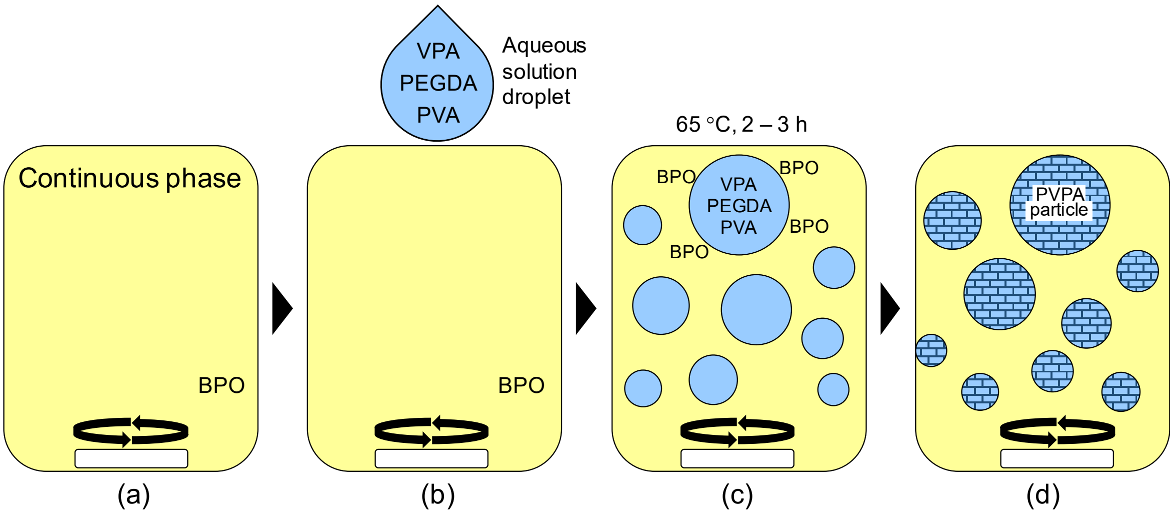

Figure 1. Schematic illustration of the W/O suspension polymerization.

The synthesis conditions are shown in Table 1.

Table 1. Synthesis conditions of crosslinked PVPA particles.

Sample name	Monomer (VPA)	Crosslinker (PEGDA)	Stabilizer (PVA)	Initiator (BPO)
PVPA-5	12.7 mmol	5% mole ratio of VPA	0.01% mole ratio of VPA	1% mole ratio of VPA
PVPA-10		10% mole ratio of VPA		
PVPA-15		15% mole ratio of VPA		
PVPA-20		20% mole ratio of VPA		
PVPA-30		30% mole ratio of VPA		

2.3 Determination of metal ion concentrations

A sample solution, a complexing reagent solution, and a buffer solution were mixed and absorption spectra in the visible region were measured at 10 min after the addition of the complexing reagent with a spectrophotometer (V-570, JASCO). As for the complexation reactions of 5-Br-PAPS with Cu^{2+} or Zn^{2+}, pH was 8 and absorbances at 558 nm was used for their determination [23]. As for CPA-III with La^{3+}, Tb^{3+}, or Lu^{3+}, pH was 1.2, and absorbances at 667.5 nm was used [24-26]. In all cases, calibration curves were made with standard metal ion solutions.

2.4 Batch adsorption study

The pH of initial metal ion solutions was adjusted to 1 – 6 with 1.0 mol L^{-1} HCl or 1.0 mol L^{-1} NaOH solution. The PVPA particles (20 mg) and each of the metal ion solutions (10 mL) were added into a glass vessel and then it was shaken on an orbital shaker (300 rpm) for a period of time at room temperature (25 ± 2 °C).

The amount of metal ions adsorbed per unit weight of adsorbent, q_{eq} in mol g^{-1}, and the percent extraction ($\%E_{\mathrm{A}}$) were calculated using the following equations:

$$q_{\mathrm{eq}} = \frac{(C_0 - C_{\mathrm{eq}})V}{m} \qquad (1)$$

$$\%E_{\mathrm{A}} = \frac{C_0 - C_{\mathrm{eq}}}{C_0} \times 100 \qquad (2)$$

where C_0 is the initial metal ion concentration (in mol L^{-1}), C_{eq} is the metal ion concentration at equilibrium (in mol L^{-1}), V is the volume of the solution (in L), and m is the weight of the PVPA particles (in g). The equilibrium pH was also measured and it was used for the following analyses.

In most experiments, the initial metal ion concentrations were not higher than 1.0×10^{-4} mol L^{-1}. Under these conditions, metal hydroxide precipitation does not occur in the pH range of 1 – 6 [27] for the five metal ions used.

3. Results and Discussion

3.1 Synthesis of crosslinked poly(vinylphosphonic acid) particles

3.1.1 Selection of organic continuous phase

Taylor investigated the size of liquid emulsions in another liquid (continuous phase), and proposed the following equation to describe the deformation of emulsions dynamically [28]:

$$\frac{L-B}{L+B}=\frac{Ga\eta}{2\gamma}\frac{19\eta_{\mathrm{i}}+16\eta}{16\eta_{\mathrm{i}}+16\eta} \quad (3)$$

where G is the shear rate (in s^{-1}), η and η_{i} are the viscosities (in Pa s) of the continuous phase (oil) and the dispersed liquid (water), respectively, and γ is the interfacial tension (in N m^{-1}) at the oil/water interface. Fast speed stirring produces higher G values. Initially, spherical water droplets are formed in the oil continuous phase, the radius of which is a. When the oil continuous phase is stirred, the water droplet shape changes from spherical to ellipsoidal. L and B are the lengths of the major and minor axes of the ellipsoid, respectively. When the left-hand side of eq. (3) is small, $L \approx B$ and water droplets will keep their spherical shape. When the left-hand side is large, $L >> B$ and water droplets are deformed. This deformation results in the formation of smaller droplets by tearing off the ellipsoid edges. Therefore, higher η and smaller γ cause smaller droplets with the same stirring speed.

Kwak *et al.* used toluene as the continuous phase [15], and thus we also used toluene to synthesize PVPA particles by the W/O dispersion polymerization at first. However, PVPA particles were not formed by our instruments. We attempted to synthesize PVPA particles with the other five solvents with high viscosity in Table 2. As the result, PVPA particles were successfully synthesized with three silicone oils, but not with toluene, cyclohexanol, and 2-ethyl-1,3-hexanediol. The viscosity of KF-96-100CS is between those of cyclohexanol and 2-ethyl-1,3-hexanediol. Therefore, the success in KF-96-100CS and the failures in cyclohexanol and 2-ethyl-1,3-hexanediol cannot be explained only by viscosity.

Table 2. Organic solvents used and their viscosity.

Name	Viscosity / mPa s	Name	Viscosity / mPa s
Toluene	0.560 (25 °C)*	KF-96-100CS	96.2 (25 °C)**
Cyclohexanol	41.067 (30 °C)*	KF-96-1000CS	967 (25 °C)**
2-Ethyl-1,3-hexanediol	323 (20 °C)*	KF-96-3000CS	2900 (25 °C)**

*Ref. 29, **Ref. 30.

Equation (3) includes the interfacial tension (γ), which is a factor to be considered. In general, γ at alcohol/water interfaces is small and γ at hydrophobic silicone oil/water interfaces is expected to be large. Therefore, γ is also not a decisive factor from eq. (3). Alcohols are known to show interfacial activity. As mentioned above, BPO would work as an initiator at the interface of the W/O suspension. Therefore, the polymerization could not proceed with cyclohexanol and 2-ethyl-1,3-hexanediol because these alcohols were adsorbed at the interface.

It is important that these silicone oils were found to be suitable for the W/O suspension polymerization in the present study. In the following, we used the PVPA particles synthesized with KF-96-100CS because KF-96-100CS has a lower viscosity and is more easily washed away from the particles.

3.1.2 Effects of crosslinker PEGDA

Since polymers were expected to swell, gel, or dissolve in a solvent without a crosslinker, PEGDA was added as a crosslinker. The crosslinker is also important for maintaining particle shape. If the crosslinker concentration is too high, the porosity of the particles will be lost or the particles will bind together [31]. Therefore, it is desirable to keep the crosslinker concentration low.

As shown in Figure 2, the synthesis yield of PVPA increased slightly with the increase in the PEGDA content. Kesenci [20], Tuncel [21], and Senel [32] also found that the synthesis yield was affected by the crosslinker concentration. Although the synthesis yield is low, PVPA-10 was used in the following because it has the highest adsorption capacity, which will be discussed later.

3.2 Characterization of PVPA particle

3.2.1 Fourier transform infrared (FT-IR) spectra

Figure 3 shows the FT-IR spectra of synthesized PVPA particles. The broad and weak signal appearing at 3600 – 3100 cm^{-1} and multiple signals around 2160 – 1946 cm^{-1} are attributed to the O-H and P-OH of VPA, respectively. The signals at 1724 and 1264 cm^{-1} are due to the C=O and C-O stretchings of PEGDA, respectively. The signal at 1264 cm^{-1} is also due to the P=O stretching of PVA. The signals at 1085 – 1000 and 938 cm^{-1} are attributed to the P=O and P-OH stretching, respectively [33]. The FT-IR spectra do not change significantly with changing PEGDA content. However, the C=O signal at 1724 cm^{-1} is more pronounced with the higher PEGDA content. The FT-IR results proved that the PVPA particles were successfully synthesized.

3.2.2 Particle shape and size

Figure 4(a) shows optical microscope images of the synthesized PVPA particles with a stirring speed of 400 rpm. They are spherical. The size distribution of these particles was made with all microscope images and is shown in Figure 5(a). They are 20 – 254 µm in size and polydispersed. Particles synthesized by this suspension polymerization are known to be polydispersed [18,19]. This may be caused by the inhomogeneity of the stirring speed, that is, the inhomogeneity of G in eq. (3), by location.

3.2.3 Surface morphology

Since the particle surface cannot be observed in detail by optical microscopy, the particles were measured by SEM. SEM images of the PVPA particles are shown in Figure 6. The surface of PVPA-5 seems to be smooth. The images suggest that the roughness

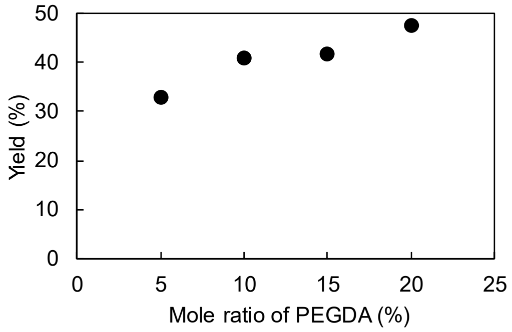

Figure 2. The effect of the crosslinker content on the synthesis yield.

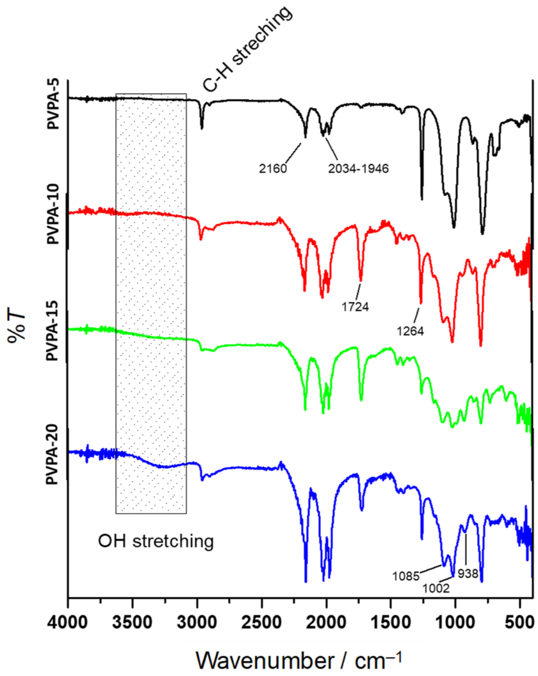

Figure 3. FT-IR spectra of the PVPA particles. The vertical axis is shifted for easier viewing.

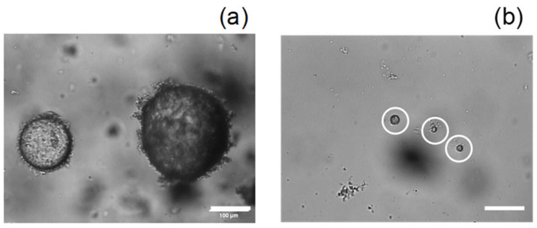

Figure 4. Optical microscope images of PVPA-10 particles with a stirring speed of (a) 400 rpm and (b) 700 rpm. White scale bars correspond to 100 µm.

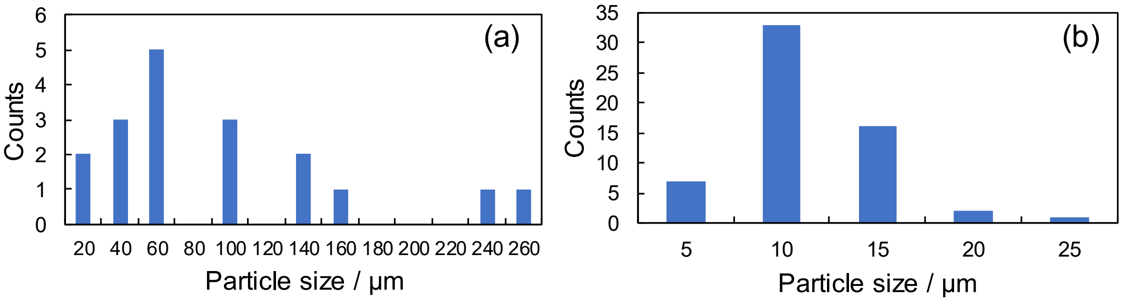

Figure 5. Size distribution of PVPA-10 particles with a stirring speed of (a) 400 rpm and (b) 700 rpm.

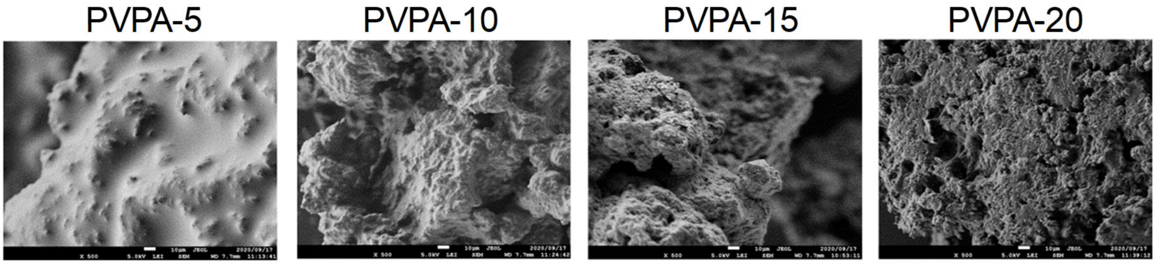

Figure 6. SEM images of the PVPA particles. White scale bars correspond to 10 µm.

and porosity of the PVPA surface increase with the increase in the crosslinker. This may be caused because the higher content of the crosslinker results in more shrinkage during polymerization.

3.3 Metal ion adsorption

Preliminary experiments on the adsorption equilibrium time showed that the equilibrium was almost attained after a shaking time of 1.5 h, and therefore most of the following experiments were conducted with a shaking time of 2 h or longer.

3.3.1 Effect of crosslinker PEGDA

The effect of the crosslinker PEGDA content on the Tb^{3+} adsorption efficiency is shown in Figure 7. Since this experiment was preliminary, it was conducted with a short shaking time (30 min) and pre-equilibrium $\%E_A$ values were obtained. PVPA-5 shows the smallest $\%E_A$ value due to its smooth surface. The $\%E_A$ values decreased with the increase in the PEGDA content among PVPA-10 to PVPA-20. This may be due to the fact that the VPA content decreases with the increase in the PEGDA content. PVPA-10 showed the highest adsorption capacity and it was employed in the following experiments.

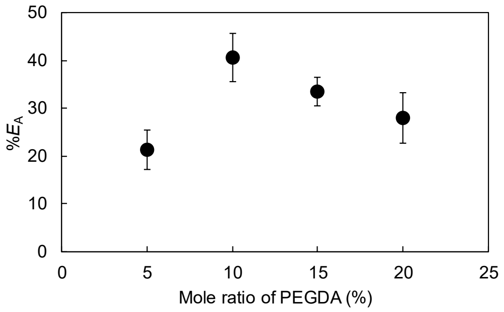

Figure 7. Effect of the crosslinker PEGDA content on the extraction of Tb^{3+}. Initial Tb^{3+} concentration 1.0×10^{-5} mol L^{-1}, pH 1.47 – 1.50, shaking time 30 min.

3.3.2 Effect of pH

The effects of pH on the extraction of metal ions were investigated in the pH range of 1 – 6. Higher pH was not investigated due to the precipitation of metal hydroxides [27]. Figure 8 displays the adsorption of Tb^{3+}; it is clear that the adsorption of Tb^{3+} onto PVPA-10 depends on pH. A similar pH dependence was observed for all other metal ions. This is explained by the deprotonation of phosphonic acids of the PVPA particles.

In order to obtain more detailed information about the adsorption equilibrium, the distribution ratio for adsorption, D_A, was calculated with the following equation:

$$D_A = \frac{q_{eq}}{C_{eq}} = \frac{C_0 - C_{eq}}{C_{eq}} \frac{V}{m} \qquad (4)$$

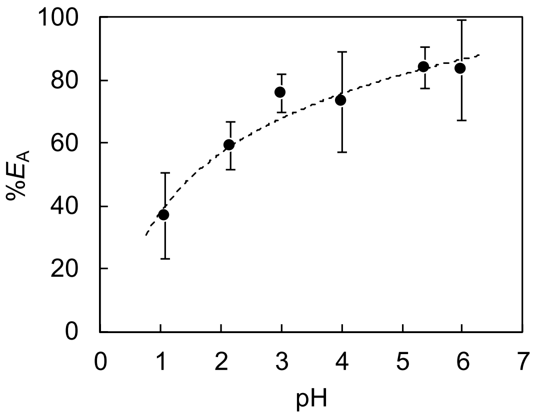

Figure 8. Effect of pH on the extraction of Tb^{3+} with PVPA-10. Initial Tb^{3+} concentration 5.0×10^{-5} mol L^{-1}, shaking time 4 h.

Different from the distribution ratio for the solvent extraction, D_A has a unit of L g^{-1}. The adsorption equilibrium of metal ion (M^{n+}) is expected to be:

$$M^{n+} + m\overline{HA} \overset{K_A}{\rightleftarrows} \overline{MA_m^{(n-m)+}} + mH^+ \qquad (5)$$

where K_A is the equilibrium constant of eq. (5), HA is a phosphonic acid functional group of PVPA, and the upper bar means solid phase. D_A can be written as:

$$\log D_A = \log \frac{[\overline{MA_m^{(n-m)+}}]}{[M^{n+}]} = \log K_A + \log[\overline{HA}]^m + m\text{pH} \qquad (6)$$

where [ ] of the upper bar species means the amount of the species per unit weight of PVPA (in mol g^{-1}) and is the same definition as q_{eq}.

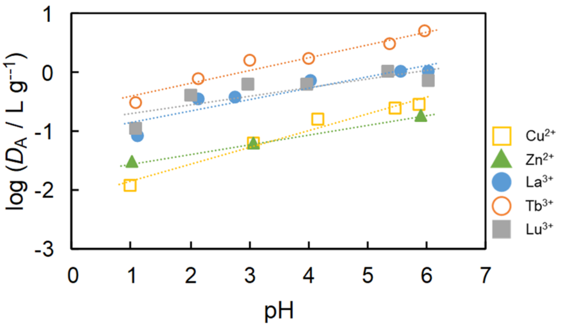

Figure 9. Dependence of log D_A on pH with PVPA-10. Initial metal ion concentrations 5.0×10^{-5} mol L^{-1}. Shaking time 2 h for Cu^{2+}, Zn^{2+}, and 4 h for La^{3+}, Tb^{3+}, Lu^{3+}.

Figure 9 displays plots of log D_A as a function of pH. The plots show almost linear relations for all metal ions. The slope values obtained by the least-squares method were 0.28, 0.16, 0.20, 0.22, and 0.15 for Cu^{2+}, Zn^{2+}, La^{3+}, Tb^{3+}, and Lu^{3+}, respectively, which correspond to the m values in eq. (6). These values also correspond to the binding ratios of the metal ions to $\overline{HA}$, that is, 1 : m. In the solvent extraction systems, the slope of the log D versus pH plot is almost equal to the charge number of the metal ion. This is due to the fact that organic solvents have a much lower permittivity and the charge number of an extracted metal complex should be zero. The slope values of Figure 9 were much smaller than the charge numbers of the metal ions in the present case. This is probably because the PVPA particles are hydrophilic and they were immersed in the aqueous solutions, which allows the partial charge neutralization.

It is necessary to consider the influence of the change of $\overline{[\mathrm{HA}]}$ with pH on the plots of log D_A versus pH in eq. (6) because the phosphonic acid group shows acid-dissociation. It is known that the acid-dissociation of polymers depends on the degree of dissociation (α) due to the electrostatic interaction. From the acid-dissociation curve of PVPA, it was found that $\alpha \approx 0.15$, 0.25, and 0.37 at pH 4.0, 5.0, and 6.0, respectively [34]. Calculations using these α values showed that the influence of α on the plot of log D_A versus pH was almost within the symbol size, and hence its influence is negligible.

From the intercepts of Figure 9, log K_A + log $\overline{[\mathrm{HA}]}^m$ values were calculated to be –2.1, –1.7, –1.1, –0.6, and –0.8, for $\mathrm{Cu^{2+}}$, $\mathrm{Zn^{2+}}$, $\mathrm{La^{3+}}$, $\mathrm{Tb^{3+}}$, and $\mathrm{Lu^{3+}}$, respectively. The values for $\mathrm{La^{3+}}$, $\mathrm{Tb^{3+}}$, and $\mathrm{Lu^{3+}}$ are larger than those for $\mathrm{Cu^{2+}}$ and $\mathrm{Zn^{2+}}$. This would be due to the difference in electrostatic interaction caused by the difference in the charge number. The $\overline{[\mathrm{HA}]}$ value cannot be obtained at this stage. If all of the phosphonic acid groups of PVPA are involved in the adsorption, the maximum $\overline{[\mathrm{HA}]}$ value was calculated to be 7.4×10^{-3} mol g^{-1} from the molecular weights of VPA and PEGDA and their reaction ratios. However, the realistic $\overline{[\mathrm{HA}]}$ value should be smaller than this value, because only the phosphonic acid groups in the surface region are involved in the adsorption.

Since the separation ability of the metal ions used in the present study is high in the solvent extraction using phosphoric acid diester or alkylphosphonic acid monoester, in which the charges of the metal ions are completely neutralized, we consider that the main reason for the low separation ability is the partial charge neutralization as shown in Figure 9. As mentioned above, this partial charge neutralization would occur because the PVPA particles are too hydrophilic compared with organic solvents of solvent extraction.

3.3.3 Saturated adsorption capacity and its improvement

Figure 10 shows the adsorption isotherm of $\mathrm{Cu^{2+}}$ onto PVPA-10 particles. It shows a saturation curve, and therefore the data were fitted to the following Langmuir isotherm by the nonlinear least-squares method:

$$q_\mathrm{eq} = \frac{q_\mathrm{sat} K C_\mathrm{eq}}{1 + K C_\mathrm{eq}} \qquad (7)$$

where K and q_sat are the adsorption constant (in L mol^{-1}) at $C_\mathrm{eq} \rightarrow 0$ and saturated q_eq, respectively. q_sat value was obtained as 1.3×10^{-5} mol g^{-1}. The q_sat value for $\mathrm{In^{3+}}$ of PVPA synthesized by Kwak *et al.* was reported to be about 5×10^{-4} mol g^{-1} [15], which was larger than ours.

In order to enlarge the q_sat value, the following improvements were carried out for PVPA-10 with KF-96-100CS.

1) BPO was hard to dissolve in the silicone oil. Thus, BPO was first dissolved in 2 mL of toluene and then added to 20 mL of the silicone oil.

2. The stirring speed during the synthesis was increased from 400 rpm to 700 rpm to synthesize smaller particles.

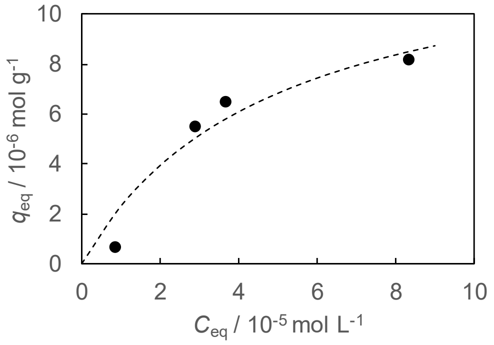

Figure 10. Adsorption isotherm of $\mathrm{Cu^{2+}}$ onto PAPV-10 particles. pH 5 – 6, shaking time 2 h. The broken line indicates the fitting curve of eq. (7).

3. The synthesized particles were washed three times with toluene and three times with methanol because

the silicone oil might remain on the surface and inside of the particles.

4. During the above washing process, sonication was done for 5 min to wash away the silicone oil.

Figure 4(b) and Figure 5(b) show the microscope images and size distribution of the synthesized PVPA-10 particles. The above improvements clearly reduced the size of the particles, which were 5 – 25 μm.

Since the monomer, crosslinker, initiator, continuous phase, and the synthesis temperature were almost the same, and only the stirring speed and the washing process were different, the chemical properties of PVPA particles are considered to be almost the same. Therefore, in the following experiments, only experiments on the saturated adsorption capacity were conducted.

Figure 11 shows the adsorption isotherms of Cu^{2+} and La^{3+} onto the revised PVPA-10 particles. In these experiments, the initial metal ion concentrations were higher than 1.0×10^{-4} mol L^{-1} and thus the possibility of metal hydroxide precipitation was calculated for each experimental condition. As a result, it was confirmed that no metal hydroxide precipitation occurred under any conditions. The obtained q_{sat} values for Cu^{2+} and La^{3+} were 4.5×10^{-5} and 1.8×10^{-4} mol g^{-1}, respectively. The Cu^{2+} q_{sat} value was 3.5 times larger than the previous one. It is difficult to compare the q_{sat} values of In^{3+} and La^{3+} directly because of the different metal ions. However, the q_{sat} value of La^{3+} is not so different from that of In^{3+} [15].

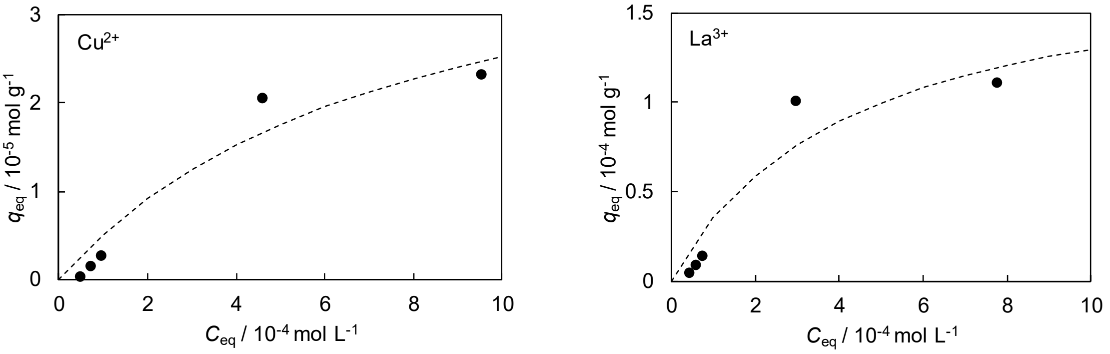

Figure 11. Adsorption isotherms of Cu^{2+} and La^{3+} onto the revised PVPA-10 particles. pH 5 – 6, shaking time 2 h. The broken lines indicate the fitting curves of eq. (7).

4. Conclusion

In the present study, three silicone oils of different viscosities were used as the continuous phase (oil) in the W/O suspension polymerization for the first time, and crosslinked PVPA particles were successfully synthesized in all silicone oils. We attempted to synthesize PVPA particles with other three organic solvents for the continuous phase, but were not successful in any solvents. These results were discussed using the physical properties of the solvents and Taylor's equation. The adsorption properties of metal ions (Cu^{2+}, Zn^{2+}, La^{3+}, Tb^{3+}, and Lu^{3+}) onto the synthesized PVPA particles were comparable to those to PVPA synthesized by other methods. Therefore, the W/O suspension polymerization using silicone oils found in the present study is a promising method for the synthesis of other particles in the future.

It is expected that more detailed characterization of the surface and internal properties of the particles will lead to deeper discussions on the adsorption of metal ions. Based on the results of the present study, more hydrophobic particles with the same functional groups would give better separation ability in the future.

Acknowledgement

This study was supported by Researcher Development Project in Basic Science, Monbukagakusho Honor Scholarship for Privately-Financed International Students from JASSO, and Matsuda Yosahichi Memorial Foreign Student Scholarship.

References

1) A. Valerie, A. Garbine, B. Laurent, *Eur. Pat. Appl.,* **17**, 1-18 (2019).
2) R. E. Dey, I. Wimpenny, J. E. Gough, D. C. Watts, P. M. Budd, *J. Biomed. Mater. Res., Part A,* **106**, 255-264 (2018).
3) J. A. Bonham, M. A. Faers, J. S. van Duijneveldt, *Soft Matter,* **10**, 9384-9398 (2014).
4) Z. Dai, T. Ngai, *J. Polym. Sci., Part A: Polym. Chem.,* **51**, 2995-3003 (2013).
5) R. A. Meurer, *Angew. Chem.,* **56**, 7380-7386 (2017).
6) K. Naseem, Z. H. Farooqi, M. Z. U. Rehman, M. A. U. Rehman, M. Ghufran, *Rev. Chem. Eng.,* **35**, 285-309 (2019).
7) M. Ahmaruzzaman, *Adv. Colloid Interface Sci.,* **166**, 36-59 (2011).
8) B. L. Rivas, E. Pereira, P. Gallegos, D. Homper, K. E. Geckeler, *J. Appl. Polym. Sci.,* **92**, 2917-2922 (2004).
9) I. Komasawa, T. Otake, Y. Higaki, *J. Inorg. Nucl. Chem.*, **43**, 3351-3356 (1981).
10) F. Nakashio, K. Kondo, A. Murakami, Y. Akiyoshi, *J. Chem. Eng. Jpn.*, **15**, 274-279 (1982).
11) F. Zhang, J. Dai, A. Wang, W. Wu, *Inorg. Chim. Acta*, **466**, 333-342 (2017).
12) A. Kaltbeitzel, *Solid State Ionics,* **178**, 469-474 (2007).
13) V. Najafi, K. Kabiri, F. Ziaee, H. Omidian, M. J. Zohuriaan-Mehr, H. Bouhendi, H. Farhadnejad, *J. Polym. Res.,* **19**, 9866 (7 pages) (2012).
14) N.-S. Kwak, H. M. Park, T. S. Hwang, *Chem. Eng. J.,* **191**, 579-587 (2012).
15) N.-S. Kwak, Y. Baek, T. S. Hwang, *J. Hazard. Mater.,* **203-204**, 213-220 (2012).
16) N. Sahiner, *Water, Air, Soil Pollut.,* **225**, 1982 (8 pages) (2014).
17) I. Anil, S. T. Gunday, A. Bozkurt, O. Alagha, *Nanomaterials,* **10**, 131 (23 pages) (2020).
18) R. Arshady, *Colloid Polym. Sci.,* **270**, 717-732 (1992).
19) E. Vivaldo-Lima, P. E. Wood, A. E. Hamielec, A. Penlidis, *Ind. Eng. Chem. Res.,* **36**, 939-965 (1997).
20) K. Kesenci, E. Piykin, *Macromol. Chem. Phys.,* **199**, 385-391 (1998).
21) A. Tuncel, *Colloid Polym. Sci.,* **278**, 1126-1138 (2000).
22) B. C. Melo, F. A. A. Paulino, V. A. Cardoso, A. G. B. Pereira, A. R. Fajardo, F. H. A. Rodrigues, *Carbohydr. Polym.*, **181**, 358-367 (2018).
23) D. Horiguchi, M. Saito, K. Noda, K. Kina, *Anal. Sci.*, **1**, 461-465 (1985).
24) T. Taketatsu, M. Kaneko, N. Kono, *Talanta*, **21**, 87-91 (1974).
25) T. Taketatsu, *Bull. Chem. Soc. Jpn.*, **50**, 1758-1761 (1977).
26) G. Jinzhang, Z. Xiangming, K. Jingwan, B. Guangbi, *Anal. Lett.*, **18**, 1507-1517 (1985).
27) C. F. Baes, Jr., R. E. Messmer, "*The Hydrolysis of Cations*", Wiley-Interscience, New York (1976).
28) G. Taylor, *Proc. R. Soc. London, Ser. A*, **146**, 501-523 (1934).
29) J. A. Riddick, W. B. Bunger, "*Organic Solvents*", 3rd ed., Wiley-Interscience, New York (1970).

30) https://www.silicone.jp/products/type/oil/detail/search/straight.shtml

31) P. J. Dowding, B. Vincent, *Colloids Surfaces A Physicochem. Eng. Asp.,* **161**, 259-269 (2000).

32) S. Senel, H. Cicek, A. Tuncel, *J. Appl. Polym. Sci.,* **67**, 1319-1334 (1997).

33) B. H. Stuart, "*Infrared Spectroscopy: Fundamentals and Applications*", John Wiley & Sons, Inc., Hoboken (2005).

34) B. Bingöl, W. H. Meyer, M. Wagner, G. Wegner, *Macromol. Rapid Commun.*, **27**, 1719-1724 (2006).